corrosion and materials degradation

MDPI

Article

An Experimental and Computational Approach for the Utilization of Expired Escitalopram as a Corrosion Inhibitor for Carbon Steel

Abdur Rahman [1], Salma Bilal [1], Salma Gul [1,*], Shamsa Munir [2], Javaria Sadaf [1] and Bakhtiar Ali [3,*]

[1] National Centre of Excellence in Physical Chemistry, University of Peshawar, Peshawar 25120, Pakistan; abdurrahmankp75@gmail.com (A.R.); salmabilal@uop.edu.pk (S.B.); javariaktk9305@gmail.com (J.S.)
[2] Industrial Sciences Research Labs, National University of Technology, Islamabad 44000, Pakistan; smunir@nutech.edu.pk
[3] School of Engineering and Built Environment, Griffith University, Nathan, QLD 4111, Australia
* Correspondence: salmagul@uop.edu.pk (S.G.); dralibakhtiar@gmail.com (B.A.)

Abstract

Corrosion of carbon steel in acidic medium remains a major industrial concern, requiring efficient and economical corrosion inhibitors. In this work, expired Escitalopram was examined as a potential waste-derived corrosion inhibitor for carbon steel in 1 M HCl using experimental and computational approaches. The protection efficiency increased with inhibitor concentration but decreased with elevated temperature, indicating an adsorption-controlled inhibition mechanism. The optimum inhibition efficiency of 97.34% was determined at 150 ppm after 4 h immersion at 25 °C through gravimetric analysis. Similar behaviour was demonstrated through potentiodynamic polarization (PDP), where an efficiency of ~97% was recorded at 150 ppm. In EIS analysis, charge-transfer resistance increased with inhibitor concentration. Thermodynamic and kinetic parameters were evaluated to elucidate the inhibition mechanism. Surface characterization using SEM, EDX, and FTIR provided supporting evidence consistent with reduced surface deterioration and inhibitor–surface interaction. Computational analysis complemented the experimental results, supporting favourable adsorption of expired Escitalopram. The findings demonstrate the potential of expired Escitalopram as an effective corrosion inhibitor and a possible route for value-added reuse of expired pharmaceutical material under acidic corrosion conditions.

Keywords: carbon steel; corrosion; anti-corrosion activity; Escitalopram drug; computational study

Check for updates

Academic Editor: Bahram Vaghefinazari

Received: 8 August 2026
Revised: 26 September 2026
Accepted: 28 September 2026
Published: 1 October 2026

Copyright: © 2026 by the authors. Licensee MDPI, Basel, Switzerland. This article is an open access article distributed under the terms and conditions of the Creative Commons Attribution (CC BY) license.

1. Introduction

Carbon steel is extensively used throughout in many different sectors, including transportation infrastructure, petroleum, and construction. However, corrosion is a serious concern associated with these sectors, where it causes severe damage [1]. Corrosion emerges from electrochemical reactions where the atoms of the metal surface yield electrons to electron acceptors (acids, oxygen, or cations) present in the air or wet media. The oxidation process leads to progressive deterioration of the metal surface [2]. Corrosion is not only dangerous for metals but also affects humans, plants, animals, and the environment. Corroding metals release toxins into water and air, resulting in pollution and posing a threat to human health [3]. Corrosion costs nearly USD 2.5 trillion annually, as stated by the US National Association of Corrosion Engineers [4]. HCl is commonly used in chemical processing, iron pickling, acidification of oil wells, and boiler descaling. However, carbon

steel corrodes in HCl due to its corrosive nature towards the surface of carbon steel [5]. Therefore, the formulation and use of efficient corrosion inhibitors are important to extend the life of carbon steel components and improve operational effectiveness.

As reported by the U.S. Consumer Healthcare Products Association, Germany's Federal Ministry of the Environment and Variant Market Research's Indian data analysis, and, the Pharmaceutical companies all over the world manufacture nearly 100,000 tons of different manufactured products each year [6]. In recent decades, the market of drugs has expanded from USD 125 billion in 2016 to USD 273 billion by 2024, in which a large section of synthetic drugs remain unutilized and ultimately expire, causing pharmaceutical waste, resulting in financial losses for pharmaceutical companies and healthcare systems [7]. Beyond traditional synthetic corrosion inhibitors, growing environmental and regulatory concerns have encouraged the development of organic corrosion inhibitors derived from renewable, low-toxicity, or waste-valorised sources. Recent research has therefore explored plant extracts, biopolymers, amino acids, biomass-derived molecules, and other organic compounds containing adsorption-active heteroatoms and π-electron systems as alternatives to conventional corrosion inhibitors [8,9]. Within this broader spectrum of organic corrosion inhibitors, there has been growing interest in exploring drug-derived substances as effective corrosion inhibitors, with expired pharmaceuticals representing a distinct and increasingly studied category, primarily owing to their complex molecular structures rich in heteroatoms (S, P, N, or O) and aromatic rings, which facilitate strong adsorption onto metal surfaces [10].

Expired drugs, even though intentionally or unintentionally thrown out, have a serious effect on the environment, human beings, and aquatic conditions. To overcome such pharmaceutical waste, the expired or unused drugs can be utilized again as corrosion inhibitors for metals, mitigating both environmental and economic losses. However, expired pharmaceuticals should not be considered intrinsically environmentally benign; improper disposal of unused or expired drugs is itself an environmental and waste-management concern. Their use as corrosion inhibitors is more appropriately viewed as a potential waste-valorization strategy in which an otherwise discarded pharmaceutical material is repurposed for a functional application [11].

Recent research has explored drug-derived substances as corrosion inhibitors and has reported substantial corrosion inhibition through adsorption on metal surfaces. Nevertheless, inhibitor performance depends strongly on molecular structure, concentration, metal type, and corrosive environment. Various classes of drugs, including antibiotics, antihypertensives, antidepressants, and anti-inflammatory agents, have been evaluated as alternative corrosion inhibitors. Compounds such as Frisium [12], citalopram [13], and Eslicarbazepine acetate [14] have been reported to exhibit inhibition efficiencies exceeding 90% under specific experimental conditions, commonly attributed to adsorption of drug molecules on metal surfaces in acidic media. These findings highlight the potential of expired pharmaceuticals as alternative corrosion inhibitors while also providing an opportunity for pharmaceutical-waste valorization. To the best of our knowledge, the corrosion-inhibition performance of expired Escitalopram for carbon steel in 1 M HCl under the experimental conditions investigated in the present work has not previously been reported.

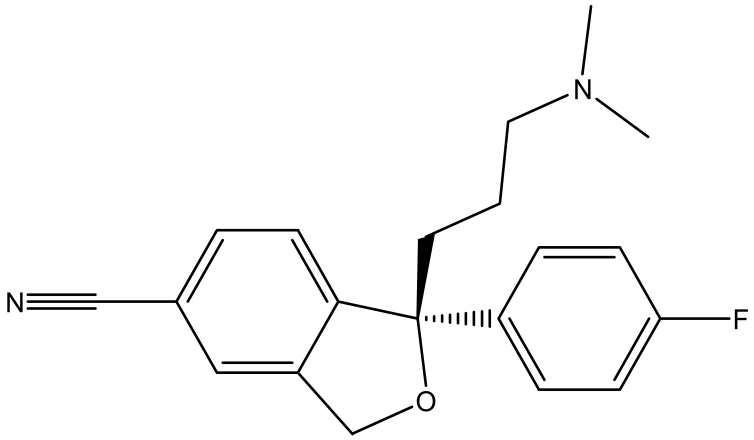
The structure of the Escitalopram drug contains π bonds, a benzene ring, and polar and non-polar groups such as amine, nitrile, and ether [15]. In this work, the expired Escitalopram was used to reduce corrosion on the surface of carbon steel in a 1 M HCl acidic solution through gravimetric analysis and electrochemical methods such as PDP and EIS. The effectiveness of expired Escitalopram as a cost-effective, pharmaceutical-waste-derived corrosion inhibitor for the surface of carbon steel in 1 M HCl was further

evaluated at various temperatures. In addition, FTIR, EDX, and SEM were used to interpret the correlation of the drug with the surface of carbon steel. To gain comprehension of adsorption and the inhibitory mechanism of the drug molecules, semi-empirical PM3 studies were employed.

2. Materials and Methods

2.1. Materials

The chemical composition of low carbon steel (CS) utilized in this study is as follows: C (0.15%), Mn (0.96%), Si (0.16%), and Fe (98.73%), respectively. The CS specimens were cut into uniform dimensions of 1 × 1 × 1 cm for smooth experimentation [16]. These coupons were polished with emery paper 400, 600, and 800 grit for a metallic shine, washed with distilled water to eliminate any contamination, and dried with acetone [17]. The 1.0 M HCl acidic medium was prepared as the corrosive solution with analytical-grade reagents (37%) by diluting the proper amount of acid in distilled water to attain the blank solution. Distilled water and methanol were used for preparation of solutions in UV-visible spectroscopy. Expired Escitalopram tablets, labelled as containing 10 mg Escitalopram per tablet, were used in this study. The tablets were ground and the required mass was calculated from the labelled API content to prepare the inhibitor solutions. Because the Escitalopram content of the expired tablets was not independently quantified by a validated chromatographic method, all inhibitor concentrations reported in this work are nominal concentrations based on the labelled API content. UV-Vis spectroscopy was used for comparative spectral characterization and not for quantitative determination of the remaining Escitalopram content. The chemical structure of the drug is displayed in Scheme 1. This drug is commonly used for the treatment of anxiety, panic, social anxiety, and obsessive–compulsive disorders [18].



Scheme 1. Chemical structure of the Escitalopram drug.

2.2. Instruments

UV-visible data were collected using a PerkinElmer spectrophotometer (PerkinElmer, Waltham, MA, USA). CS coupons were precisely weighed using a digital balance (AX 120, Shimadzu, Kyoto, Japan). The electrochemical analysis were accomplished by using a three electrode electrochemical cell with a Gamry Ref. 1010 Potentiostat/Galvanostat (Gamry Instruments, Warminster, PA, USA) in which platinum used as auxiliary/counter electrode [19], silver-silver chloride (Ag/AgCl) as reference electrode [20], and CS coupon was used as working electrode. Cary630 FTIR Spectrometer (Agilent Technologies, Santa Clara, CA, USA) was used to analyze the infrared spectra within the range of 4000–400 cm^{-1}. FTIR was used to identify the functional groups present in expired Es-

citalopram drug and the adsorbed molecules of the drug after 4 h immersion time on the surface of CS by adding the optimal concentration of 150 ppm in 1 M HCl at 25 °C. SEM and EDX analysis were carried out using the SEM (JSM5910 JEOL, Tokyo, Japan) instrumentation after 4 h time of immersion in 1 M HCl.

2.3. Methods

2.3.1. Gravimetric Analysis

Gravimetric analysis is a highly precise and proper method for the calculation of the inhibition efficiency and corrosion rates of metals. Before experimentation, the CS samples were accurately weighed using a digital balance according to ASTM G1-03, Standard Practice for Preparing, Cleaning, and Evaluating Corrosion Test Specimens [21]. Each coupon was exposed to 100 mL of test solution, with one 1 × 1 cm face exposed to the solution, corresponding to an exposed surface area of 1 cm^2. The remaining five faces were not exposed. The resulting solution-volume/surface-area ratio was 100 mL cm^{-2}. Each condition was tested using three independently prepared coupons, and the results are reported as mean ± standard deviation. After a specified period, the CS coupons were removed, rinsed with distilled water followed by acetone, dried, and precisely weighed. All the experiments were conducted at controlled temperatures ranging from 15 to 40 °C (±1 °C) using a thermostatic water bath. The potential of the expired drug in preventing carbon steel corrosion was determined by calculating the inhibition efficiency percentage (I.E %) using Equation (1), whereas surface coverage (θ) is given in Equation (2) [22]:

$$\text{I.E\%} = \frac{W_0 - W_i}{W_0} \times 100 \quad (1)$$

$$\theta = \frac{W_0 - W_i}{W_0} \quad (2)$$

where W_0 is the weight loss of metal samples with no inhibitor, and W_i is the weight loss of metal samples with inhibitor.

The corrosion rate (C_R) in mil per year is obtained through Equation (3):

$$C_R(\text{mpy}) = \frac{534 \times W}{A \times T \times D} \quad (3)$$

where C_R is the rate of corrosion (mpy), D is the density of CS (g/cm^3), T is time of immersion (h), A is the surface area of CS pieces (cm^2) and W is weight loss (mg). The inhibitor concentration ranged from 30 to 300 ppm in increments of 30 ppm to determine the optimal concentration. These values represent the nominal concentrations, calculated from the labeled active pharmaceutical ingredient (API) content of the expired Escitalopram tablets prior to dissolution; no independent analytical confirmation (HPLC) of the active Escitalopram content at the time of testing was performed. All the concentrations of the drug reported throughout this work should be understood as nominal, label-based values rather than analytically verified concentrations. Other factors were held constant to evaluate the inhibitor's efficacy for optimal results. To ascertain the optimal immersion duration, studies were conducted at varying immersion times from 1 to 7 h, with 1-h intervals between each trial. The experiments were conducted at varied temperatures, specifically 15 °C, 20 °C, 25 °C, 30 °C, 35 °C, and 40 °C, to examine the impact of temperature on the inhibitor's potency and corrosion rate.

2.3.2. Electrochemical Studies

Potentiodynamic polarization technique was executed to determine the inhibition efficiency of the inhibitor, corrosion potential, and corrosion current density, for CS with a 1 cm^2 surface area in 1 M HCl solution [5].

The efficiency of inhibition in percentage (I.E %) of the drug was determined using Equation (4).

$$\text{I.E } \% = \frac{i^{\circ}_{corr} - i_{corr}}{i^{\circ}_{corr}} \times 100 \quad (4)$$

where i°_{corr} and i_{corr} are the corrosion current in the blank and inhibited solution, respectively.

The electrochemical impedance spectroscopy (EIS) approach was utilized to evaluate the potential of expired Escitalopram as a corrosion inhibitor and its charge transfer resistance for carbon steel in a 1 M HCl solution. The surface area (θ) and the inhibition efficiency of the inhibitor were calculated using Equation (5):

$$\text{I.E } \% = \theta \times 100 = 1 - \frac{R^{\circ}_{ct}}{R_{ct}} \times 100 \quad (5)$$

where R°_{ct} and R_{ct} are the charge transfer resistances of the blank and inhibited solution, respectively.

2.3.3. Computational Studies

The computational study was performed using the semi-empirical PM3 method in HyperChem 8.0.10 software. The molecules were optimized and single-point energy calculations were performed to obtain the total energies, energies of HOMO/LUMO and graphical representation and location of these orbitals. To represent steel, a 1 × 1 × 1 Fe crystal was built using the crystal builder option. The single-point energy calculations were performed on individual molecules and then on the Escitalopram–Fe crystal adsorption complex to obtain the adsorption energy [23]. The interaction tendency of water with the adsorption complex of Escitalopram–Fe crystal was also evaluated through single-point energy calculations. DFT studies were also performed using the 3-21G basis set in HyperChem 8.0.10 software.

3. Results and Discussion

3.1. Spectroscopic Analysis

UV-visible spectroscopy technique was employed for structural characterization of the non-expired and expired Escitalopram drug. To obtain the spectra, 80% *v*/*v* methanol AR grade (Merck, Darmstadt, Germany) in distilled water was used as a reference solvent [24]. The non-expired and expired drugs (150 ppm) exhibited absorption bands at similar wavelengths, while the expired drug showed lower absorbance under the measurement conditions. This difference may reflect changes associated with storage or degradation; however, UV-Vis measurements alone do not permit quantitative determination of the remaining Escitalopram content. The peak at 238 nm might be assigned to π→π* transitions of aromatic C=C chromophores present in the phenyl rings (Figure 1) of the drug molecule [25]. This transition reflects the high electron density within the conjugated system, which facilitates the adsorption onto the surface of carbon steel through π-electron transitions. The second peak observed at 283 nm corresponds to n→π* transitions [26], involving the lone pair electrons on atoms of nitrogen. These heteroatoms, particularly nitrogen, play a significant role in the corrosion inhibition by donating electron density to the vacant d-orbitals of the carbon steel, resulting in the formation of a protective adsorbed layer. The presence of both electron-donating heteroatoms and π-electron systems enhances the potential for the

adsorption of Escitalopram drug on the surface of CS, thereby improving its inhibition efficiency as a corrosion inhibitor. The FTIR analysis was done for expired drug and CS adsorbed with expired drug in HCl solution (Figure 1b). In the FTIR analysis, expired drug and molecules of the drug adsorbed on CS show peaks at 3374 and 3411 cm^{-1}, indicating O-H stretching [27], 2107 and 2111 cm^{-1}, indicating C≡N stretching [28,29], and 1545 and 1672 cm^{-1}, showing C=C stretching [30], as shown in Figure 1b, which confirms that the molecules of the inhibitor are adsorbed on the CS surface [31].

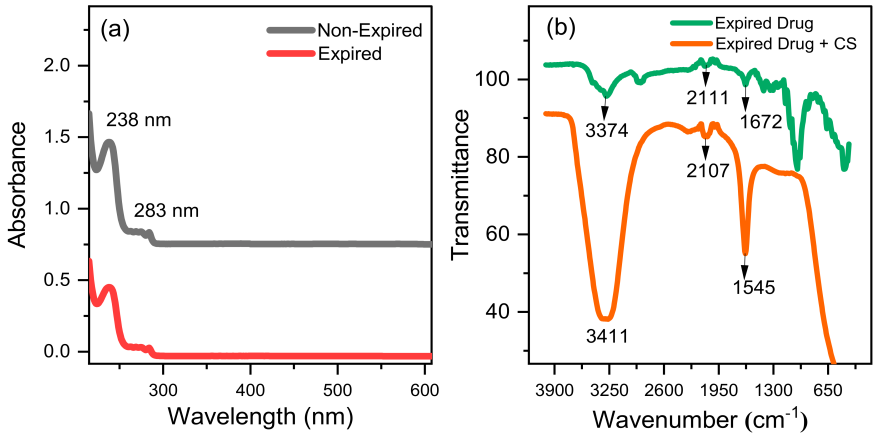


Figure 1. (**a**) UV-visible spectra of non-expired and expired Escitalopram drug (150 ppm). (**b**) The FTIR spectra of expired Escitalopram with and without adsorption on CS.

3.2. Gravimetric Analysis

The inhibitory effect of the drug was evaluated by varying its concentration from 30–300 ppm in 1 M HCl at various temperatures. All inhibitor concentrations reported in this work are nominal concentrations calculated from the labelled API content of the expired tablets. The weight loss was measured after keeping the CS in 1 M HCl for the duration of 7 h after each hour. The I.E was obtained using Equation (1) given in the methods section (see Figure 2a–f). The optimal protection efficiency was obtained at a concentration of 150 ppm of expired drug in 1 M HCl. This phenomenon can be attributed to greater adsorption of inhibitor molecules onto the carbon steel surface. I.E did not increase further even when the inhibitor concentration was increased up to 300 ppm and remained almost the same as at 150 ppm. This can be attributed to the absence of active sites for adsorption on the CS surface, and as a result, the surface of the adsorbent becomes saturated.

As seen in Figure 2, the I.E % of expired drug increased to ~97% at 150 ppm when the time of immersion increased from 1 h to 4 h; however, a decline was noted in the I.E % when the time of immersion increased from 4 h to 7 h [32]. This effect can be best explained by a donor–acceptor interaction between the single-paired electrons on the donor atom of Escitalopram drug and the vacant d-orbitals of the iron atoms [33]. Figure 3 shows the weight loss of carbon steel at different inhibitor concentrations and immersion times over the investigated temperature range (15–40 °C). As shown in Figure 3, the weight loss of carbon steel increased with immersion time at all temperatures, while increasing the inhibitor concentration considerably reduced the weight loss.

The plot of corrosion rates obtained at different temperatures vs. inhibitor concentration is shown in Figure 4. Increasing the temperature above 25 °C decreased the inhibition efficiency and increased the corrosion rate. The corrosion of carbon steel involves the metal's dissolution along with the evolution of hydrogen in an acidic solution. A rise in temperature escalates the cathodic hydrogen evolution reactions, which act as an effective electron-consuming cathodic reaction. Moreover, higher temperatures also facilitate desorption of inhibitor molecules from the carbon steel specimen surface. As a result, a

greater portion of the CS surface becomes uncovered to the acidic solution, resulting in an increased corrosion rate as shown in Figure 4a–f. The rise in temperature not only increases the rate of metal dissolution but also reduces the potency of the inhibitor by encouraging desorption from the surface of CS [34].

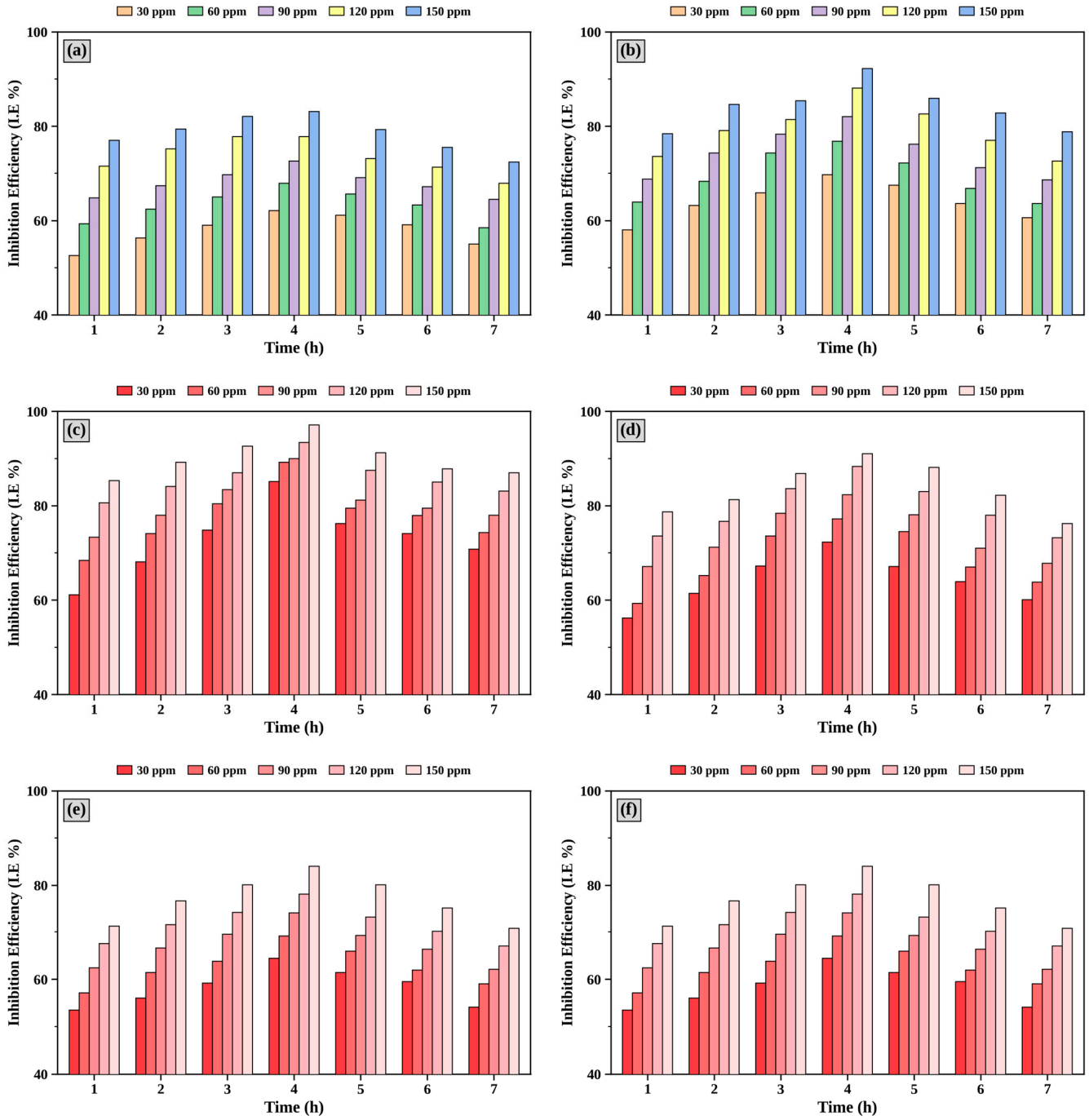


Figure 2. Corrosion inhibition efficiency (I.E.) calculated at various concentrations of drug for CS in 1 M HCl solution at (**a**) 15 °C, (**b**) 20 °C, (**c**) 25 °C, (**d**) 30 °C, (**e**) 35 °C, and (**f**) 40 °C for 1–7 h immersion time.

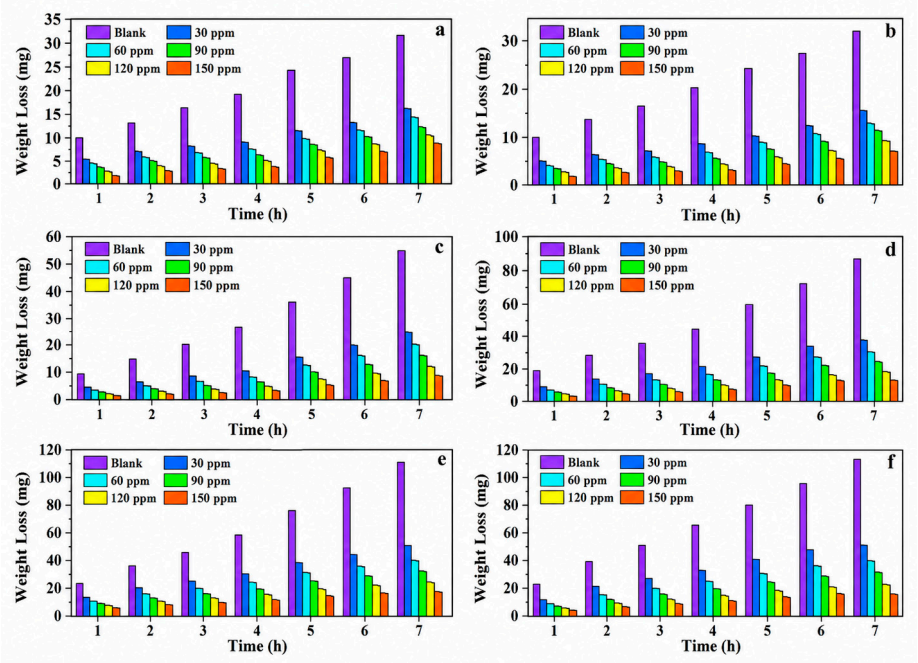


Figure 3. Weight loss of CS in 1 M HCl solution in the presence and absence of different inhibitor concentrations at (**a**) 15 °C, (**b**) 20 °C, (**c**) 25 °C, (**d**) 30 °C, (**e**) 35 °C, and (**f**) 40 °C for (1–7 h) immersion time.

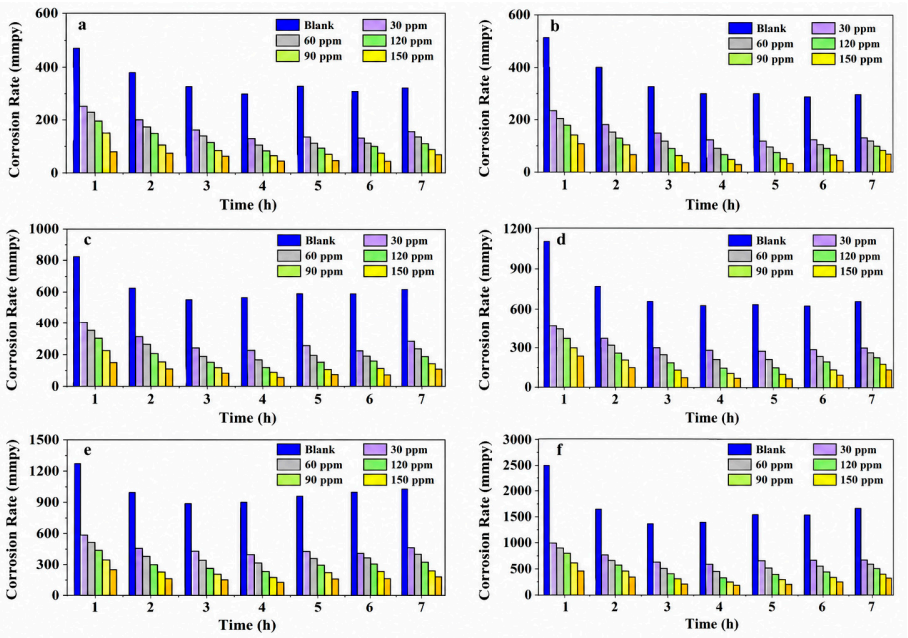


Figure 4. Corrosion rate versus inhibitor concentrations (30 to 150 ppm) at (**a**) 15 °C, (**b**) 20 °C, (**c**) 25 °C, (**d**) 30 °C, (**e**) 35 °C, and (**f**) 40 °C for (1–7 h) immersion time.

3.3. Adsorption Studies

Adsorption isotherms provide valuable insights into the interaction between the inhibitor molecules and the surface of the metal. The adsorption behavior of the inhibitor was examined using the Temkin (Equation (6)), Langmuir (Equation (7)), and Freundlich (Equation (8)) adsorption isotherm models. The surface-coverage data were linearized using the appropriate form for each model: θ versus ln C for Temkin Figure 5a, C/θ versus C for Langmuir Figure 5b, and ln θ versus ln C for Freundlich Figure 5c. The corresponding regression coefficients (R^2) and fitted parameters of the Temkin, Langmuir, and Freundlich adsorption models at each investigated temperature are given in Table 1. The Langmuir

model showed consistently high regression coefficients (R^2 = 0.986–0.998); however, the fitted slopes ranged from 1.111 to 1.466 and therefore deviated from the ideal value of unity. These deviations indicate non-ideal adsorption behaviour and suggest that the assumptions of equivalent adsorption sites and negligible interactions between adsorbed species may not be fully satisfied. The relatively high R^2 values obtained for the Temkin and Freundlich models further indicate that these models also provide reasonable descriptions of the adsorption data. Therefore, the Langmuir model is considered an approximate representation rather than evidence of strictly ideal Langmuir adsorption and was used for the subsequent thermodynamic interpretation. The equations for the three models studied are given below:

$$\text{Temkin: } \theta = (1/f) \ln K_{Ads} + (1/f) \ln C \quad (6)$$

$$\text{Langmuir : } \frac{C}{\theta} = \frac{1}{KAds} + C \quad (7)$$

$$\text{Freundlich: } \ln \theta = \ln K_{ads} + n \ln C \quad (8)$$

Table 1. Temkin, Langmuir and Freundlich adsorption isotherms parameters for expired Escitalopram on carbon steel in 1 M HCl at various temperatures.

TEMKIN ADSORPTION PARAMETERS				
TEMPERATURE (K)	Slope	R^2	K_ads	ΔG°_ads (kJ mol^{-1})
288	1.326	0.984	182.42	−32.96
293	1.283	0.989	165.73	−32.99
298	1.281	0.991	148.54	−32.22
303	1.215	0.892	134.84	−32.51
308	1.153	0.991	122.62	−32.11
313	1.139	0.994	109.55	−33.14
LANGMUIRADSORPTIONPARAMETERS				
TEMPERATURE (K)	Slope	R^2	K_ads	ΔG°_ads (kJ mol^{-1})
288	1.466	0.996	187.39	−33.01
293	1.158	0.986	151.04	−32.76
298	1.111	0.998	135.55	−32.83
303	1.237	0.995	124.86	−32.99
308	1.344	0.994	111.45	−32.92
313	1.432	0.996	110.11	−33.41
FREUNDLICH ADSORPTION PARAMETERS				
TEMPERATURE (K)	Slope	R^2	K_ads	ΔG°_ads (kJ mol^{-1})
288	0.781	0.982	67.55	−30.21
293	0.757	0.987	53.66	−30.29
298	0.771	0.988	37.81	−32.44
303	0.784	0.985	34.62	−30.58
308	0.802	0.989	27.76	−30.73
313	0.846	0.987	21.64	−30.84

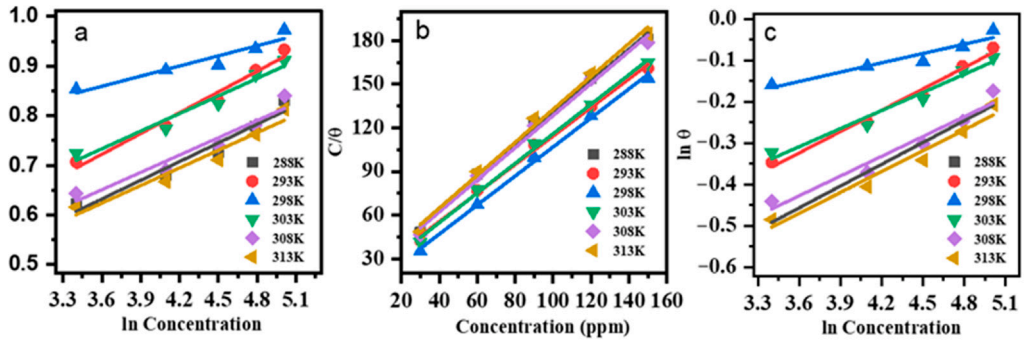


Figure 5. Linearized adsorption-isotherm plots for nominal expired Escitalopram concentration on carbon steel in 1 M HCl at different temperatures: (**a**) Temkin, θ versus ln C; (**b**) Langmuir, C/θ versus C; and (**c**) Freundlich, ln θ versus ln C.

The values of negative ΔG°_{ads} of the Langmuir adsorption isotherm, ranging from −32.76 to −33.41 kJ mol^{-1}, show that the process of adsorption is thermodynamically favorable and spontaneous. Generally, the values of ΔG°_{ads} around −20 kJ mol^{-1} or less negative are associated with physisorption involving electrostatic interactions, while the values around −40 kJ mol^{-1} or more negative are characteristic of chemisorption involving charge transfer or covalent bonding. In the current study, the values of ΔG°_{ads} are between −20 and −40 kJ mol^{-1}, suggesting that the mechanism by which the molecules of the inhibitor are adsorbed on the surface of carbon steel is mixed-type, with contributions from electrostatic interactions between the charged molecules of the inhibitor and the surface of the metal and possible donor–acceptor interactions.

3.4. Kinetic-Thermodynamic Corrosion Parameters

For the kinetic and thermodynamic investigation of the process of corrosion, the Arrhenius-type equation was employed to determine the apparent activation energy (E_a*), entropy of activation (ΔS*), and enthalpy of activation (ΔH*) with various concentrations of the investigated expired Escitalopram drug compound at temperatures ranging from 15–40 °C (288–313 K). The Arrhenius equation is expressed as Equation (9):

$$\log k_{corr} = \left(\frac{-E_a*}{2.303RT}\right) + \log A \quad (9)$$

where R represents the universal gas constant, A represents the Arrhenius pre-exponential factor, and T is absolute temperature (K). The E_a* values were attained by plotting log k_{corr} versus 1/T, which produced straight lines with a slope equal to $\left(\frac{-E_a*}{2.303RT}\right)$. From this slope, the values of E_a* were obtained. The enthalpy of activation (ΔH) and entropy of activation (ΔS) were evaluated by applying Equation (10):

$$\begin{aligned} &\log(CR/T) = \log(R/Nh) + \Delta S^*/(2.303R) - \Delta H^*/(2.303RT); \\ &\text{Slope} = -\Delta H^*/(2.303R); \\ &\text{Intercept} = \log(R/Nh) + \Delta S^*/(2.303R), \end{aligned} \quad (10)$$

where N is Avogadro's number and h is Planck's constant. The enthalpy of activation (ΔH*) and entropy of activation (ΔS*) were determined from the transition-state plot of log(CR/T) versus 1/T. The slope of the linear plot is equal to −ΔH*/2.303R, while the intercept is equal to $[\log\left(\frac{R}{Nh}\right) + \frac{\Delta S*}{2.303R}]$. The calculated kinetic and thermodynamic parameters are summarized in Table 2. The increase in Ea* in the inhibited solutions indicates that the inhibitor increases the apparent kinetic barrier for carbon-steel dissolution [35]. The rise in ΔH* values with expired drug suggested that the addition of the expired drug to the acidic

solution improves the energy threshold of the corrosion reaction; this may be assigned to the energy barrier formation over the process of corrosion. Furthermore, the negative values of ΔS* at lower inhibitor (30–120 ppm) concentrations indicate a decrease in disorder during the formation of the activated complex, proposing that the activated state represents an association process rather than a dissociation process. At higher inhibitor concentration (150 ppm), the slight positive ΔS* (+9.8 J mol^{-1} K^{-1}) value indicates increased randomness due to strong adsorption and displacement of water molecules from the surface of carbon steel [36]. The corresponding Arrhenius plots of log CR versus 1/T are shown in Figure 6.

Table 2. Activation parameters for carbon steel dissolution in 1 M HCl containing different concentrations of Escitalopram inhibitor.

Concentration (ppm)	Activation Parameters			
	E_a* (kJ mol^{-1})	ΔH* (kJ mol^{-1})	ΔS* (J mol^{-1} K^{-1})	ΔG* (kJ mol^{-1})
30	56.3	53.8	−22.0	60.4
60	59.1	56.6	−14.6	61.0
90	60.0	57.5	−12.8	61.3
120	63.6	61.1	−3.4	62.1
150	68.6	66.1	9.8	63.2

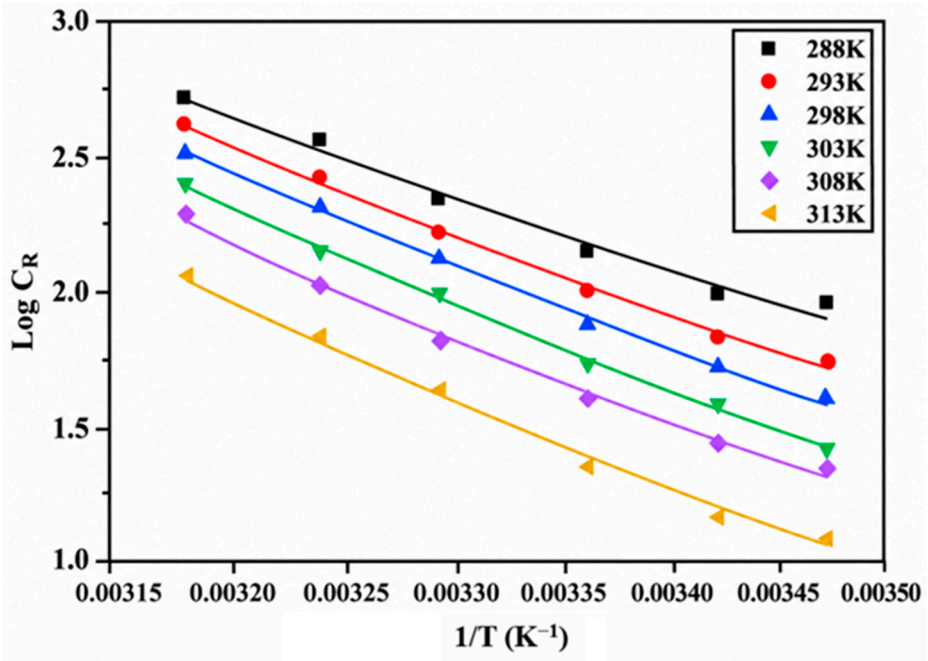


Figure 6. Arrhenius plots of log C_R versus 1/T for carbon steel in 1 M HCl containing various expired Escitalopram concentrations after 4 h immersion.

The standard free energy of adsorption was calculated from the adsorption equilibrium constant using Equation (11):

$$\Delta G^{\circ}_{ads} = -RT \ln(55.5K_{ads}) \quad (11)$$

where R is the gas constant, T is the absolute temperature and 55.5 mol L^{-1} is the molar concentration of water.

The Gibbs free energy of activation (ΔG) was obtained using Equation (12):

$$\Delta G^* = \Delta H^* - T\Delta S^* \quad (12)$$

The ΔG* values increased from 60.4 to 63.2 kJ mol^{-1} when the concentration of the inhibitor increased from 30 to 150 ppm, showing that the concentration of the drug raises the energy barrier for the process of corrosion. Overall, the increase in activation parameters such as E_a, ΔH, ΔS, and ΔG* describes the energy barrier and kinetics of the reaction of corrosion itself, not the thermodynamics of the inhibitor adsorption.

3.5. Electrochemical Analysis

3.5.1. Potentiodynamic Polarization

Figure 7 depicts the curves of potentiodynamic polarization for CS immersed in 1 M HCl at various temperatures (15–40 °C), in blank and in the presence of different concentrations of expired Escitalopram drug. Before polarization, the working electrode was maintained at open-circuit potential for 30 min until a stable potential was obtained [37]. Polarization scans were recorded from 250 mV below OCP to 250 mV above OCP at a scan rate of 1 mV/s. An exposed area of 1.0 cm^2 was used, and each measurement was repeated three times; the reported electrochemical parameters are expressed as mean ± standard deviation. For determination of the Tafel slopes, the approximately linear portions of the cathodic and anodic branches were fitted over potential ranges between −100 and −50 mV and between +50 and +100 mV relative to E_{corr}, respectively. The polarization curves were obtained to visualize the impact of the inhibitor's constituents adsorbed on the cathodic and anodic peaks of the polarization curve. The primary polarization attributes attained using the Tafel extrapolation technique, such as corrosion potential (E_{corr}), the corrosion current density (i_{corr}), cathodic Tafel slope (βc) and anodic Tafel slope (βa), are summarized in Table 3. In addition, the inhibition efficiency (I.E %) at various concentrations (30–150 ppm), obtained from the values of i_{corr}, is displayed in Table 3. Similar to gravimetric analysis, the data demonstrate that raising inhibitor concentration from 30 ppm to 150 ppm gradually reduces i_{corr}, implying the inhibition of CS decomposition in the drug's presence. Meanwhile, an increase in I.E.% reveals an inverse relationship between i_{corr} and I.E.%, which is consistent with previous electrochemical corrosion studies on metallic alloys [38]. The changes observed in βa and βc indicate that the presence of expired Escitalopram alters the kinetics of both cathodic and anodic reactions, suggesting that the drug behaves as a mixed-type inhibitor [39,40].

Table 3. Parameters obtained through potentiodynamic polarization (PDP) of CS using the inhibitor drug in 1 M HCl.

Concentration (ppm)	E_{corr} (mV vs. Ag/AgCl)	I_{corr} (μAcm^{-2})	βa (mdec^{-1})	−βc (mVdec^{-1})	I.E (%)
		Temperature = 15 °C			
Blank	−384.4 ± 3.1	52.84 ± 1.15	293.7 ± 6.9	262.7 ± 6.9	--
30	−352.7 ± 2.8	18.05 ± 0.69	245.6 ± 5.9	239.8 ± 5.6	65.84 ± 1.21
60	−346.7 ± 2.7	14.90 ± 0.81	218.9 ± 5.8	216.6 ± 5.5	71.80 ± 1.29
90	−339.3 ± 2.3	11.21 ± 0.49	194.8 ± 5.1	209.3 ± 4.8	78.80 ± 1.95
120	−333.2 ± 2.1	8.96 ± 1.39	178.6 ± 4.9	199.6 ± 4.7	83.15 ± 0.85
150	−327.9 ± 3.6	6.70 ± 0.31	154.1 ± 4.7	176.1 ± 4.6	87.32 ± 0.99
		Temperature = 20 °C			
Blank	−410.0 ± 3.9	61.50 ± 1.54	343.5 ± 4.2	362.5 ± 5.4	--
30	−379.0 ± 3.3	19.82 ± 0.97	215.1 ± 4.9	245.6 ± 4.8	67.80 ± 0.99
60	−376.0 ± 3.7	17.20 ± 0.16	178.0 ± 3.8	206.3 ± 3.6	72.03 ± 1.21
90	−372.3 ± 2.9	12.27 ± 1.24	164.5 ± 4.4	189.2 ± 4.1	80.16 ± 1.87
120	−360.5 ± 2.6	8.30 ± 1.12	158.5 ± 4.7	179.1 ± 5.8	86.50 ± 2.32
150	−339.7 ± 2.3	6.12 ± 1.13	114.1 ± 5.3	156.3 ± 4.2	90.08 ± 1.73
		Temperature = 25 °C			
Blank	−427.9 ± 4.7	72.53 ± 1.41	378.2 ± 5.2	392.4 ± 4.2	--
30	−419.4 ± 3.6	16.49 ± 2.31	255.9 ± 4.7	285.9 ± 3.2	77.38 ± 1.1
60	−397.0 ± 3.1	10.40 ± 0.99	183.3 ± 2.4	236.7 ± 4.1	85.66 ± 1.9

Table 3. *Cont.*

Concentration (ppm)	E_{corr} (mV vs. Ag/AgCl)	I_{corr} (μAcm^{-2})	βa ($mdec^{-1}$)	−βc ($mVdec^{-1}$)	I.E (%)
90	−386.1 ± 3.7	6.77 ± 1.11	178.1 ± 2.1	195.1 ± 2.4	90.76 ± 0.8
120	−379.2 ± 4.4	4.83 ± 2.31	168.9 ± 3.3	189.4 ± 2.9	93.38 ± 1.9
150	−364.9 ± 5.1	2.23 ± 1.99	134.7 ± 3.1	176.8 ± 1.9	96.96 ± 2.2
		Temperature = 30 °C			
Blank	−445.5 ± 3.8	79.52 ± 2.11	396.9 ± 7.1	382.3 ± 4.2	--
30	−432.7 ± 4.5	22.80 ± 3.60	345.7 ± 2.9	298.2 ± 3.3	71.32 ± 2.3
60	−406.5 ± 5.2	16.70 ± 6.15	278.4 ± 3.3	236.7 ± 2.9	78.99 ± 1.9
90	−389.4 ± 5.6	12.15 ± 3.42	194.8 ± 4.2	219.6 ± 3.3	84.78 ± 1.3
120	−377.5 ± 4.9	8.74 ± 3.27	178.8 ± 3.8	199.5 ± 1.9	89.05 ± 2.9
150	−369.2 ± 4.3	6.90 ± 1.13	147.9 ± 4.4	146.8 ± 3.7	91.32 ± 1.3
		Temperature = 35 °C			
Blank	−461.4 ± 2.9	85.77 ± 2.23	393.7 ± 3.6	376.4 ± 2.3	--
30	−439.6 ± 3.2	28.91 ± 3.17	285.9 ± 2.9	345.9 ± 2.1	66.30 ± 1.1
60	−421.9 ± 3.9	24.80 ± 4.63	284.2 ± 3.3	316.7 ± 3.8	71.08 ± 1.9
90	−418.5 ± 5.4	20.11 ± 3.20	244.8 ± 3.7	269.8 ± 4.6	76.56 ± 0.8
120	−398.1 ± 2.9	17.88 ± 2.11	198.3 ± 3.1	219.5 ± 3.4	79.24 ± 1.1
150	−383.3 ± 1.1	12.41 ± 2.94	174.8 ± 2.8	186.9 ± 3.1	85.54 ± 1.3
		Temperature = 40 °C			
Blank	−498.4 ± 3.2	94.50 ± 1.23	387.5 ± 3.1	387.9 ± 3.4	--
30	−469.2 ± 1.9	35.82 ± 2.31	297.2 ± 2.8	292.4 ± 5.1	62.32 ± 0.9
60	−441.6 ± 4.4	31.70 ± 1.91	238.7 ± 5.2	236.7 ± 3.3	66.45 ± 1.3
90	−432.8 ± 3.2	27.47 ± 1.33	214.4 ± 3.8	199.1 ± 1.8	71.00 ± 2.1
120	−427.4 ± 2.8	21.43 ± 1.92	198.6 ± 2.9	185.6 ± 4.2	77.35 ± 1.9
150	−426.2 ± 2.1	17.30 ± 3.73	152.7 ± 4.1	169.8 ± 3.9	81.69 ± 0.8

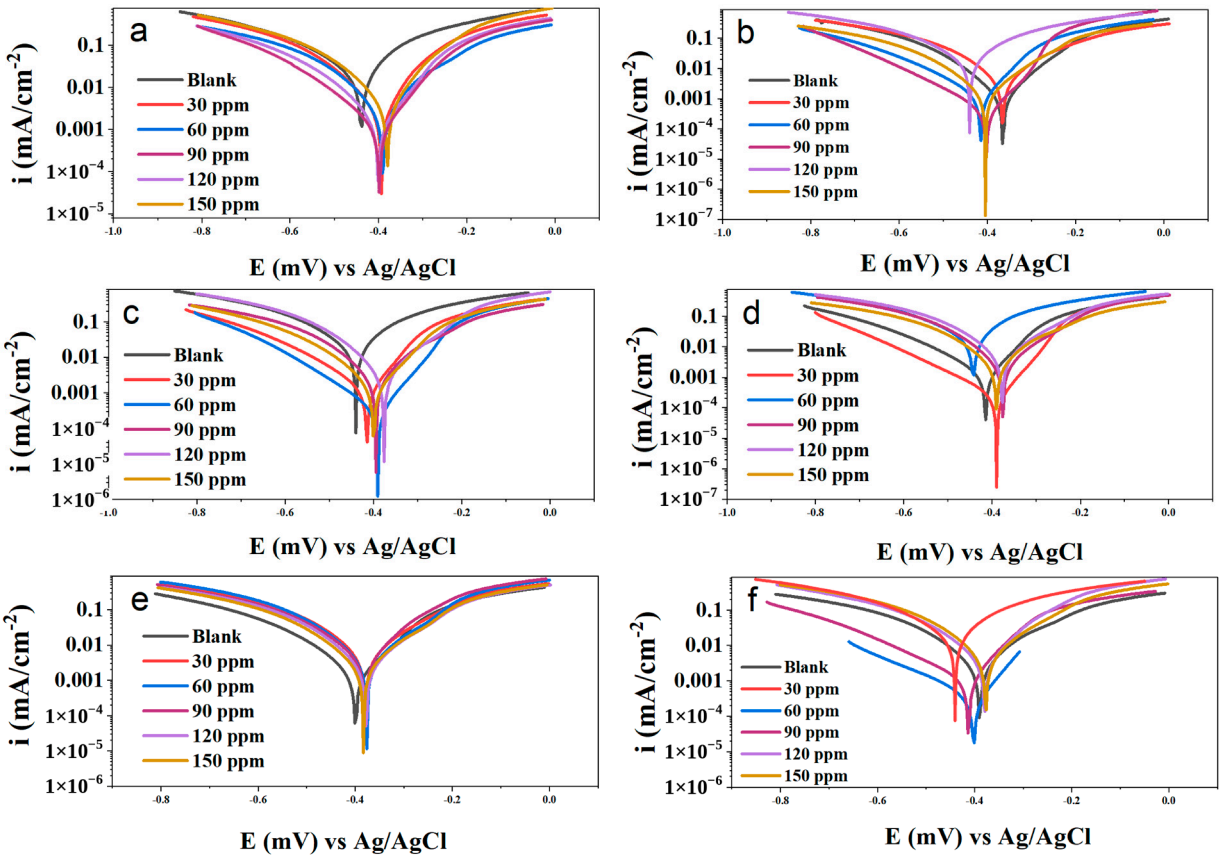


Figure 7. Polarization curves of Carbon Steel working electrode with and without various concentrations (30–150 ppm) of expired drug in 1 M HCl medium at (**a**) 15 °C, (**b**) 20 °C, (**c**) 25 °C, (**d**) 30 °C, (**e**) 35 °C and (**f**) 40 °C.

3.5.2. EIS Measurements

EIS tests were conducted to examine the behavior of corrosion of the immersed CS coupons without and with various inhibitor's concentrations (30 to 150 ppm) of expired drug in 1 M HCl acidic solution at 15–40 °C, respectively. As the concentrations of the inhibitor increased, as shown in Figure 8, the semicircle diameter also increased, which shows high charge transfer resistance (R_{ct}), implying more protection to the surface of carbon steel [41,42]. EIS tests were performed over a frequency range of 10^5 Hz to 10^{-2} Hz with an amplitude of 5 mV under open-circuit conditions [16]. The impedance spectra were fitted using Gamry Echem Analyst with the Rs–(Rct||CPE) equivalent circuit shown in Figure 8g. Equivalent-circuit fitting was performed by minimizing the χ^2 function representing the weighted residuals between the experimental and calculated impedance spectra. The fitted parameters Rs, Rct, CPE magnitude (Y_0), CPE exponent (n), and goodness-of-fit parameter (χ^2) are reported in Table 4. The surface coverage (θ) and inhibition efficiency (I.E.%) were subsequently calculated from the fitted Rct values. The double-layer capacitance (Cdl) was calculated from the fitted CPE parameters using the following equation:

$$Cdl = Y_0 (\omega_{max})^{n-1} \quad (13)$$

where $\omega_{max} = 2\pi fmax$ is the angular frequency corresponding to the maximum of the imaginary impedance component.

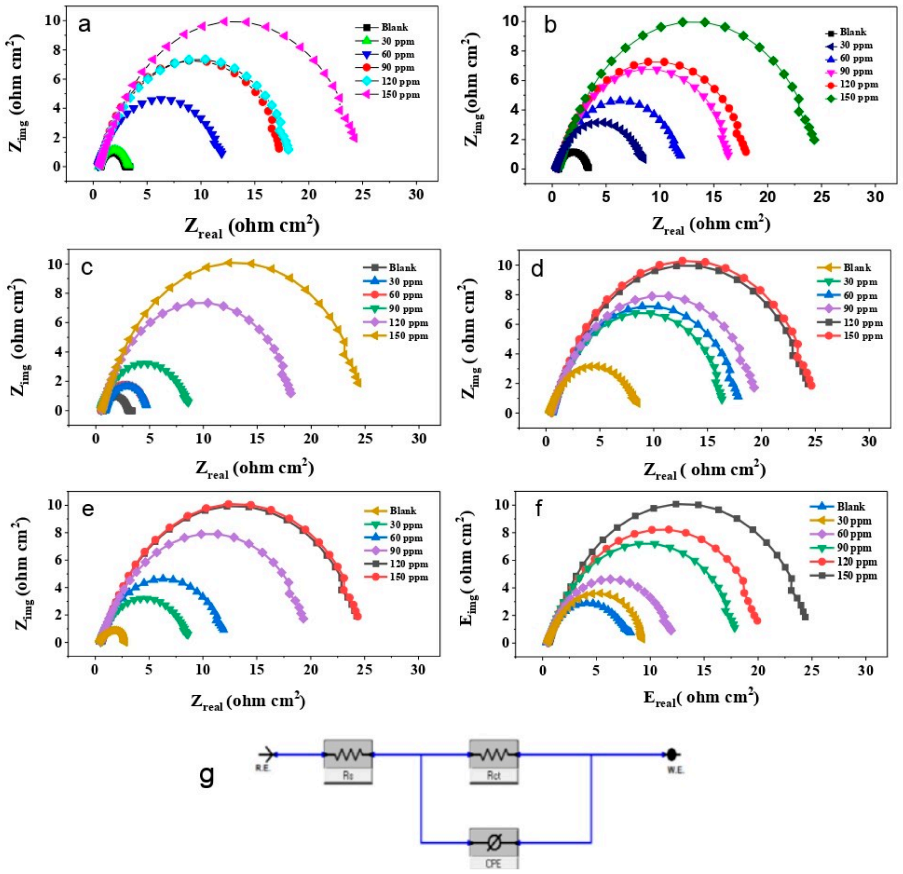


Figure 8. Nyquist curves of CS in 1 M HCl in blank and presence of various inhibitory drugs at various temperatures: (**a**) 15 °C, (**b**) 20 °C, (**c**) 25 °C, (**d**) 30 °C, (**e**) 35 °C, (**f**) 40 °C, (**g**) circuit diagram for evaluation of EIS values.

Table 4. Parameters obtained through EIS of the CS working electrode at various drug concentrations in 1 M HCl Solution.

Concentration (ppm)	R_s	R_{ct} (Ohm cm^2)	Qdl/Y_0 ($\times 10^{-4}$)	Cdl (μF/cm^2)	n	$\chi^2 \times 10^{-3}$	θ	I.E %
				Temperature = 15 °C				
Blank	0.387 ± 0.121	19.2 ± 1.8	5.284 ± 0.43	69.88 ± 2.1	0.919 ± 0.01	4.24 ± 0.66	---	---
30	0.598 ± 0.133	94.1 ± 2.3	4.917 ± 0.91	51.74 ± 3.5	0.876 ± 0.03	2.48 ± 0.43	0.796 ± 0.013	79.6 ± 1.3
60	0.632 ± 0.321	131.9 ± 2.5	4.621 ± 0.32	49.24 ± 3.1	0.851 ± 0.02	2.19 ± 0.32	0.855 ± 0.023	85.5 ± 2.3
90	0.643 ± 0.123	172.6 ± 2.1	3.678 ± 0.38	41.65 ± 3.4	0.778 ± 0.04	1.92 ± 0.76	0.889 ± 0.016	88.9 ± 1.6
120	0.687 ± 0.333	257.2 ± 2.3	2.658 ± 0.36	38.10 ± 4.6	0.769 ± 0.01	1.56 ± 0.22	0.926 ± 0.017	92.6 ± 1.7
150	0.693 ± 0.329	365.4 ± 3.1	1.481 ± 0.39	35.88 ± 2.1	0.732 ± 0.02	1.33 ± 0.64	0.948 ± 0.012	94.8 ± 1.2
				Temperature = 20 °C				
Blank	0.388 ± 0.210	23.6 ± 2.1	6.239 ± 0.29	76.29 ± 2.9	0.885 ± 0.05	4.98 ± 0.54	---	---
30	0.622 ± 0.421	118.9 ± 2.4	5.388 ± 0.87	72.65 ± 1.8	0.852 ± 0.04	2.89 ± 0.77	0.802 ± 0.019	80.2 ± 1.9
60	0.686 ± 0.323	169.8 ± 2.6	4.972 ± 0.71	68.28 ± 2.1	0.837 ± 0.01	2.65 ± 0.98	0.862 ± 0.028	86.2 ± 2.8
90	0.725 ± 0.312	243.6 ± 1.7	3.949 ± 0.43	61.65 ± 3.9	0.756 ± 0.02	2.44 ± 0.56	0.904 ± 0.014	90.4 ± 1.4
120	0.784 ± 0.414	342.5 ± 1.9	2.898 ± 0.38	55.87 ± 3.3	0.735 ± 0.04	2.21 ± 0.45	0.932 ± 0.028	93.2 ± 2.8
150	0.823 ± 0.251	478.2 ± 2.2	1.925 ± 0.71	43.98 ± 2.9	0.721 ± 0.05	1.94 ± 0.32	0.951 ± 0.031	95.1 ± 3.1
				Temperature = 25 °C				
Blank	0.399 ± 0.132	29.9 ± 1.8	7.993 ± 0.13	81.87 ± 1.5	0.878 ± 0.01	5.76 ± 0.65	---	---
30	0.654 ± 0.217	158.8 ± 2.1	6.818 ± 0.28	77.55 ± 2.1	0.841 ± 0.03	3.12 ± 0.33	0.812 ± 0.012	81.2 ± 1.2
60	0.678 ± 0.232	246.4 ± 1.7	5.176 ± 0.62	73.87 ± 1.8	0.823 ± 0.03	2.98 ± 0.88	0.879 ± 0.023	87.9 ± 2.3
90	0.699 ± 0.432	338.7 ± 1.9	4.454 ± 0.97	70.89 ± 2.3	0.722 ± 0.02	2.73 ± 0.12	0.912 ± 0.013	91.2 ± 1.3
120	0.707 ± 0.129	497.9 ± 1.2	3.626 ± 0.84	63.99 ± 1.9	0.712 ± 0.04	2.56 ± 0.17	0.940 ± 0.021	94.0 ± 2.1
150	0.793 ± 0.751	688.2 ± 2.3	2.033 ± 0.81	55.19 ± 1.2	0.707 ± 0.06	2.33 ± 0.62	0.957 ± 0.017	95.7 ± 1.7
				Temperature = 30 °C				
Blank	0.389 ± 0.121	37.8 ± 2.9	8.868 ± 0.34	87.87 ± 1.9	0.865 ± 0.07	6.32 ± 0.82	---	---
30	0.598 ± 0.122	103.5 ± 1.7	7.989 ± 0.45	81.44 ± 2.3	0.822 ± 0.09	4.11 ± 0.91	0.635 ± 0.013	63.5 ± 1.3
60	0.632 ± 0.126	144.6 ± 2.1	6.921 ± 0.31	77.43 ± 1.8	0.817 ± 0.03	3.77 ± 0.66	0.739 ± 0.024	73.9 ± 2.4
90	0.643 ± 0.111	183.9 ± 1.8	5.772 ± 0.62	72.86 ± 1.1	0.716 ± 0.04	3.44 ± 0.44	0.795 ± 0.019	79.5 ± 1.9
120	0.687 ± 0.129	219.3 ± 1.2	4.231 ± 0.32	66.92 ± 2.8	0.707 ± 0.02	3.21 ± 0.82	0.828 ± 0.022	82.8 ± 2.2
150	0.693 ± 0.231	388.2 ± 1.9	3.553 ± 0.23	61.74 ± 1.7	0.701 ± 0.05	3.01 ± 0.96	0.903 ± 0.016	90.3 ± 1.6
				Temperature = 35 °C				
Blank	0.395 ± 0.234	45.4 ± 3.9	9.793 ± 0.28	93.53 ± 2.1	0.842 ± 0.03	6.98 ± 0.81	---	---
30	0.618 ± 0.321	119.3 ± 1.2	8.798 ± 0.19	83.71 ± 1.1	0.792 ± 0.01	4.74 ± 0.24	0.620 ± 0.019	62.0 ± 1.9
60	0.644 ± 0.245	159.9 ± 2.3	7.896 ± 0.51	81.82 ± 1.8	0.786 ± 0.08	4.23 ± 0.11	0.717 ± 0.015	71.7 ± 1.5
90	0.666 ± 0.541	187.8 ± 1.9	6.983 ± 0.34	77.64 ± 1.6	0.702 ± 0.09	4.12 ± 0.62	0.759 ± 0.011	75.9 ± 1.1
120	0.691 ± 0.361	234.1 ± 2.8	5.862 ± 0.33	71.73 ± 1.5	0.691 ± 0.07	3.67 ± 0.28	0.807 ± 0.010	80.7 ± 1.0
150	0.699 ± 0.231	395.2 ± 2.7	4.687 ± 0.29	65.32 ± 1.2	0.687 ± 0.03	3.33 ± 0.71	0.886 ± 0.012	88.6 ± 1.2
				Temperature = 40 °C				
Blank	0.394 ± 0.123	58.6 ± 1.9	9.982 ± 0.21	104.69 ± 1.9	0.828 ± 0.01	7.87 ± 0.53	---	---
30	0.634 ± 0.321	133.1 ± 1.3	9.192 ± 0.11	98.62 ± 1.1	0.771 ± 0.03	5.12 ± 0.71	0.560 ± 0.013	56.0 ± 1.3
60	0.649 ± 0.122	151.9 ± 1.8	8.833 ± 0.22	87.32 ± 2.1	0.767 ± 0.02	4.72 ± 0.38	0.614 ± 0.011	61.4 ± 1.1
90	0.677 ± 0.412	177.6 ± 1.4	7.676 ± 0.28	81.39 ± 1.7	0.698 ± 0.07	4.32 ± 0.12	0.670 ± 0.021	67.0 ± 2.1
120	0.695 ± 0.227	268.2 ± 2.1	6.869 ± 0.11	77.41 ± 1.3	0.682 ± 0.06	4.29 ± 0.76	0.781 ± 0.022	78.1 ± 2.2
150	0.732 ± 0.172	371.4 ± 1.5	5.315 ± 0.27	71.87 ± 0.9	0.671 ± 0.03	4.12 ± 0.94	0.842 ± 0.027	84.2 ± 2.1

3.6. Morphological and Elemental Analyses

3.6.1. EDX Analysis

The elemental composition of both uninhibited and inhibited carbon steel was analyzed through the EDX technique following a 4-h immersion in a 1 M HCl medium at 25 °C as shown in Figure 9. The EDX analysis revealed differences in the relative elemental composition of the uninhibited and inhibited surfaces after exposure. Because EDX is semi-quantitative, these changes are interpreted as being consistent with reduced surface corrosion in the presence of the inhibitor rather than as direct proof of the composition of an adsorbed inhibitor film.

3.6.2. Scanning Electron Microscopy

Surface morphology was investigated by SEM to examine the protective effect of expired Escitalopram on the CS surface, as surface characteristics provide valuable insights into material degradation and structural stability under demanding service conditions [43,44]. The CS coupons were dipped in the blank acidic solution and in the presence of an optimum concentration of 150 ppm Escitalopram drug and then explored for sur-

face analysis. The effects are displayed in Figure 10a–c. The polished specimen showed the relatively smooth morphology expected after mechanical preparation, as shown in Figure 10a, whereas the specimen exposed to uninhibited 1 M HCl displayed pronounced surface attack, irregularities and corrosion-product deposits, as shown in Figure 10b. In comparison, the specimen exposed to the inhibited solution at nominal 150 ppm exhibited visibly less surface damage, as shown in Figure 10c. These morphological differences are consistent with the corrosion-inhibition behaviour measured by the gravimetric and electrochemical methods. SEM alone, however, does not establish the chemical composition of an adsorbed surface layer.

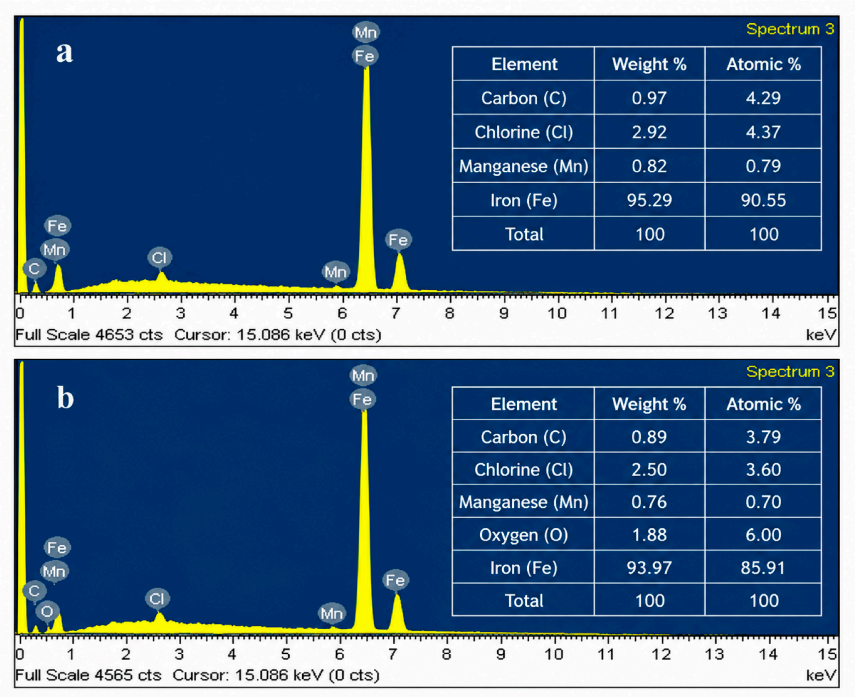


Figure 9. EDX micrographs of (**a**) CS using 150 ppm drug as inhibitor and (**b**) CS in 1 M HCl medium after 4 h immersion without adding drug inhibitor. The insets show atomic and weight percentages of elements.

3.7. Computational Analysis

Computational modeling was performed using the semi-empirical PM3 method to evaluate the drug molecules' adsorption on the four-atom Fe crystal. The computational approach complemented the experimental results by showing an effective adsorption tendency of the molecules of drug on Fe crystal. Single-point energy calculations were first performed on the individual drug molecules to obtain the energies of the highest occupied molecular orbital (E_{HOMO}) and the lowest unoccupied molecular orbital (E_{LOMO}). The graphical representation of HOMO/LUMO is shown in Figure 11. The electron affinity (EA), ionization energy (I.E) and total energy (ΔE) are correlated with LUMO and HOMO using energy Equations (14)–(16) [45,46]:

$$EA = -E_{LOMO} \quad (14)$$

$$I.E = -E_{HOMO} \quad (15)$$

$$\Delta E = E_{LOMO} - E_{HOMO} \quad (16)$$

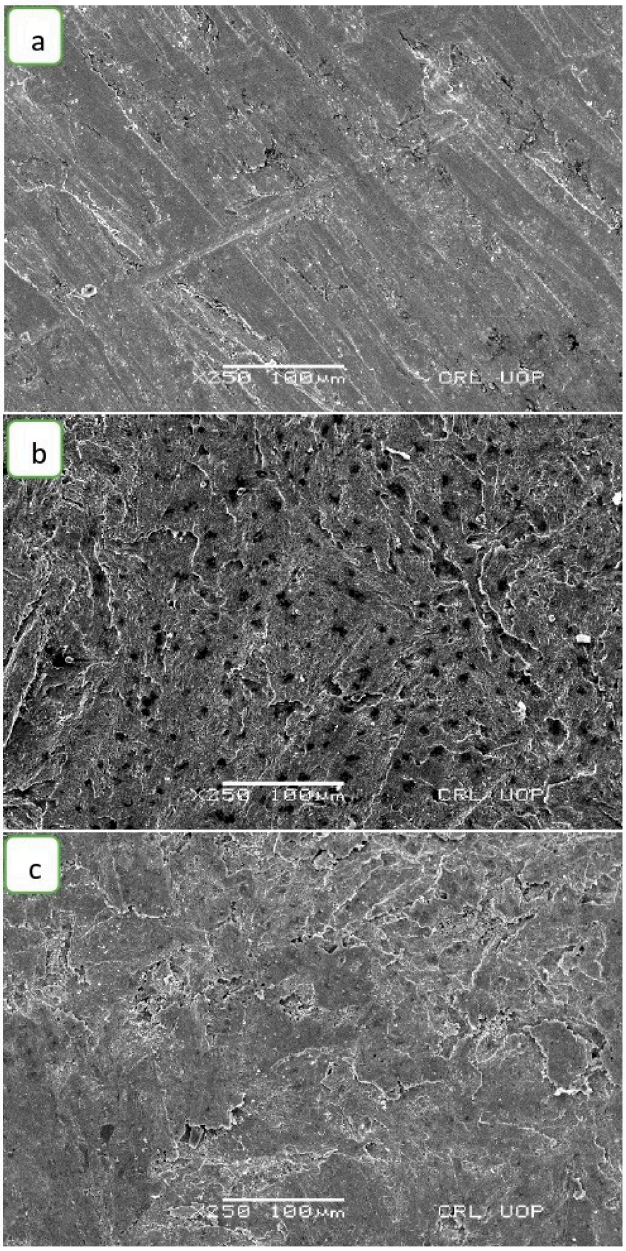


Figure 10. SEM surface morphology of (**a**) polished, (**b**) uninhibited, (**c**) inhibited CS.

Figure 11 shows the graphical representation of HOMO and LUMO for the Escitalopram drug. E_{HOMO} displays the inhibitor's capacity to give electrons to the available d-orbitals on the crystal surface [47]. On the other hand, E_{LUMO} describes molecules' capacity to receive electrons. A lower value of E_{LUMO} increases molecules' ability to receive electrons. The energy gap, ΔE, refers to the energy needed for the removal of electrons from their final occupied orbitals. Table 5 shows the parameter values determined by computational study. The adsorption energy calculations provide quantitative data regarding the favorability of the drug's binding to the surface of iron, indicating strong or weak interactions, while an analysis of changes in HOMO-LUMO energies and the dipole moment upon adsorption offers insights into the electronic reorganization occurring at the interface [48].

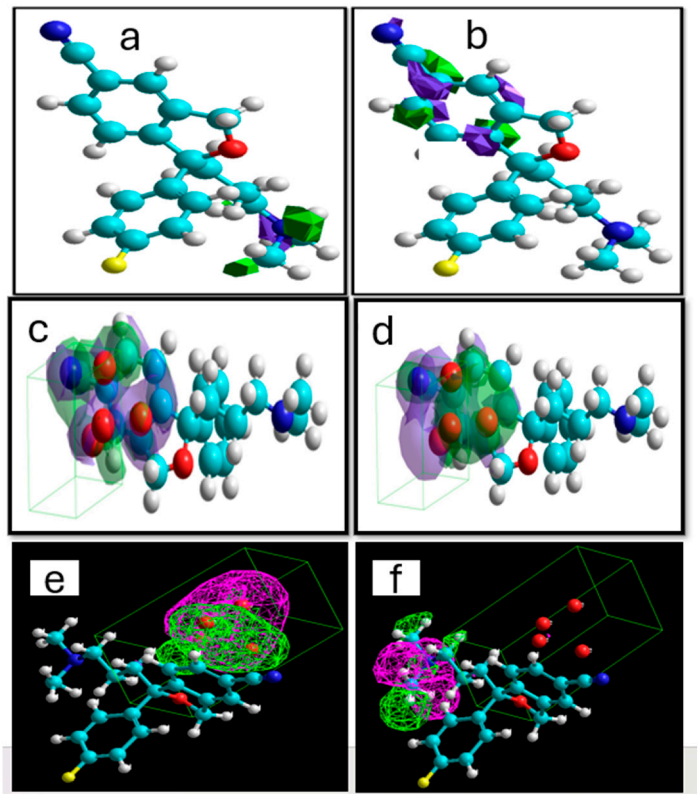


Figure 11. The graphical representation of the (**a**) HOMO and (**b**) LUMO of the drug molecule, (**c**) HOMO and (**d**) LUMO of the adsorption complex of the drug with the Fe crystal using the semi-empirical PM3 method, and (**e**) HOMO and (**f**) LUMO of the complex obtained through DFT.

Table 5. The parameters obtained through single-point energy calculations for the Escitalopram drug and the adsorption complex of the drug with the Fe crystal.

E total drug (kcal/mol)	E_{HOMO} drug (eV)	E_{LUMO} drug (eV)	$E_L - E_H$ (eV)	$E_{Ionization}$ drug (eV)	Electron Affinity drug (eV)	Electronegativity drug (eV)
−86,483.8	−9.139	−0.884	8.25	9.139	0.884	5.012
Semi-empirical Calculation of Fe crystal + Drug						
Fe (kcal/mol)	E_{drug} (kcal/mol)	$E_{Fe+drug}$ (kcal/mol)	E_{ads} (kcal/mol)	E_{HOMO} (eV)	E_{LUMO} (eV)	Dipole moment (D)
−48,537.7	−86,483.8	−135,180	−158.5	−8.252	−2.758	3.685
DFT Calculations of Fe Crystal + Drug						
−2,301,113	−569,424	−2,870,601	−64	−6.933	−4.550	30.330

The adsorption energy of the drug molecule on the Fe surface was determined using the adsorption energy calculations (using Equation (17) below):

$$E_{ads} = E_{complex} - (E_{Adsorbent} + E_{Adsorbate}) \quad (17)$$

The calculated negative adsorption energy (−158.5 kcal/mol) indicates an energetically favourable interaction between the inhibitor and the Fe model. The negative adsorption energy indicates a favourable interaction between the Escitalopram molecule and the Fe surface, supporting the experimentally observed inhibition performance [49]. The HOMO and LUMO distributions of the adsorption complex (Figure 11) suggest redistribution of electron density and possible electronic interaction between the inhibitor molecule and Fe atoms. The calculated dipole moment reflects the polarity of the modeled system and may

influence its interaction with the Fe surface. DFT calculations using the 3-21G basis set were also performed to provide additional qualitative support for the trends obtained using the semi-empirical PM3 method. The negative adsorption energy calculated for the drug-Fe complex indicates that the adsorption process is energetically favourable. Analysis of the HOMO and LUMO revealed that the drug molecule acts predominantly as the electron donor, whereas the Fe surface acts as the primary electron acceptor, suggesting favourable electronic interactions and charge transfer between the adsorbate and the Fe surface.

3.8. Mechanism of Corrosion Inhibition

The adsorption behaviour of the drug on CS is consistent with contributions from both physical and chemical interactions, as suggested by the experimental and computational results. The drug molecule contains multiple heteroatom-containing functional groups that may contribute to its interaction with the carbon steel surface, such as electron donation from the $–N(CH_3)_2$ group of the drug molecules to the unoccupied d orbitals of Fe. Theoretical studies also show the HOMO of drug molecules in this region, suggesting that the $–N(CH_3)_2$ group may represent one of the potential electron-donating sites involved in the interaction with the Fe surface. However, the adsorption thermodynamics and temperature-dependent inhibition behaviour suggest that physical adsorption may also contribute to the overall adsorption process. Initial adsorption may occur through electrostatic interactions and weak intermolecular forces. Specific interactions between electron-donating functional groups of the drug and surface Fe atoms may contribute to chemisorption, resulting in a mixed adsorption mechanism. The $–N(CH_3)_2$ group is identified as a potential electron-donating site based on the HOMO localization of the isolated drug molecule, whereas the –C≡N group becomes associated with the LUMO of the adsorbed system (as seen through DFT), indicating its potential electron-accepting character and involvement in the donor–acceptor interaction with the Fe surface.

The negative adsorption energy is consistent with favourable interaction between the inhibitor and the Fe model. Adsorption of the inhibitor molecules on the carbon steel surface is proposed to reduce access of the corrosive medium to active surface sites and thereby contribute to corrosion inhibition. The interrelationship between the inhibitor molecules and the surface of CS is described in Figure 12. The adsorption of the inhibitor molecules onto the carbon steel surface may involve interactions between electron-rich sites of the inhibitor and the vacant d-orbitals of Fe atoms [50]. As indicated by the theoretical study, the computational results suggest that the $–N(CH_3)_2$ group may contribute to adsorption through electron donation to the Fe surface.

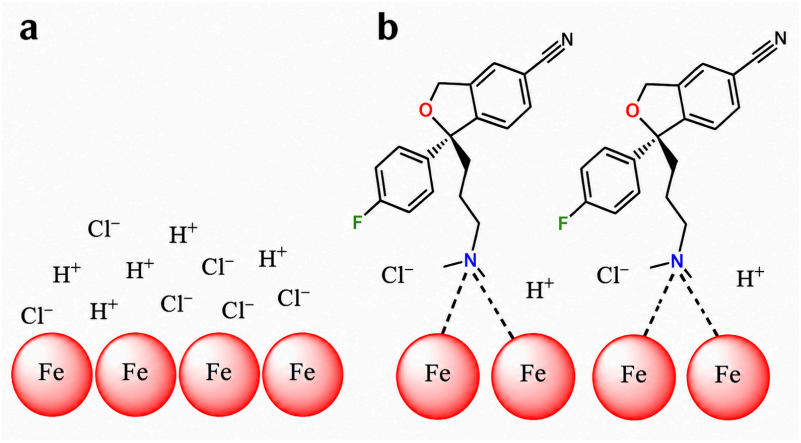


Figure 12. Proposed adsorption and inhibition against corrosion of carbon steel in 1 M HCl medium (**a**) in absence of drug and (**b**) in presence of drug.

A comparison of I.E of various drugs with our study is displayed in Table 6, where the corrosion protection efficiency of the studied molecules of the drug on the carbon steel surface is reported. It is evident that the highest corrosion inhibition has been shown by Escitalopram, which can be attributed to its high adsorption tendency on the carbon steel surface.

Table 6. Comparison of inhibition efficiencies (I.E %) of the other reported drugs with Escitalopram on CS in 1 M HCl.

Corrosion Inhibitor Drug	I.E %	Reference
Ceporex	89.3	[51]
Drotaverine	81.0	[52]
Metformin	89.4	[53]
Modazar	92.3	[54]
Dulcolax	91.8	[17]
Terconazol	80.6	[1]
Olanzapine	91.8	[55]
Podocip	96.6	[56]
Cephalexin	43.9	[57]
Cefpodoxime Proxetil	88.6	[58]
Vancomycin	94.2	[59]
Furosemide	90.5	[60]
Escitalopram	Max of ~97	This work

4. Conclusions

This study demonstrates the corrosion-inhibition potential of expired Escitalopram for carbon steel in 1 M HCl. Under the investigated conditions, the highest gravimetric inhibition efficiency was approximately 97% at a nominal concentration of 150 ppm and 25 °C. PDP and EIS measurements showed trends consistent with the gravimetric results. The adsorption analysis indicates that the Langmuir model provides a useful approximate representation of the adsorption data, although deviations of the fitted slopes from unity and the good fits obtained with other isotherm models indicate non-ideal adsorption behaviour. Adsorption thermodynamics and the overall mechanistic evidence are consistent with favourable inhibitor adsorption, with possible contributions from both physical and chemical interactions. SEM and EDX show reduced surface deterioration in the inhibited condition but are interpreted as supporting rather than definitive evidence of an adsorbed inhibitor layer. Overall, the results identify expired Escitalopram as a promising corrosion-inhibitor candidate and suggest a possible value-added reuse route for expired pharmaceutical material.

Author Contributions: A.R.: Conceptualization, visualization, data collection and analysis, and writing of the original draft. S.B., S.G., S.M., B.A. and J.S.: Conceptualization, visualization, and writing—review and editing. All authors have read and agreed to the published version of the manuscript.

Funding: This research received no external funding.

Data Availability Statement: The data sets used in this study are available upon reasonable request.

Acknowledgments: The Department of Chemistry, Women University Swabi, is gratefully acknowledged for providing research facilities.

Conflicts of Interest: The authors declare no conflict of interest.

Abbreviations

The following abbreviations are used in this manuscript:

Ag/AgCl	Silver/silver chloride reference electrode
API	Active pharmaceutical ingredient
AR	Analytical reagent (grade)
ASTM	American Society for Testing and Materials
CPE	Constant phase element
CR	Corrosion rate
CS	Carbon steel
EA	Electron affinity
EDX	Energy-dispersive X-ray spectroscopy
EIS	Electrochemical impedance spectroscopy
FTIR	Fourier-transform infrared spectroscopy
HOMO	Highest occupied molecular orbital
I.E.	Inhibition efficiency
LUMO	Lowest unoccupied molecular orbital
mpy	Mils per year
PDP	Potentiodynamic polarization
PM3	Parametric Method 3
ppm	Parts per million
R.E.	Reference electrode
SEM	Scanning electron microscopy
UV–Vis	Ultraviolet–visible spectroscopy
v/*v*	Volume per volume
W.E.	Working electrode

References

1. Abdallah, M.; Soliman, K.A.; Alfakeer, M.; Hawsawi, H.; Al-Bonayan, A.M.; Al-Juaid, S.S.; Abd El Wanees, S.; Motawea, M.S. Expired antifungal drugs as effective corrosion inhibitors for carbon steel in 1 M HCl solution: Practical and theoretical approaches. *ACS Omega* **2023**, *8*, 34516–34533. [CrossRef] [PubMed]
2. Motawea, M.M.; Younes, A.A.; Ragab, I.; Satti, A.A.; Daoub, R.M.; Bashir, S.H. One potential method of recycling expired thiocolchicoside drug is to use an environmental corrosion inhibitor for carbon steel in HCl. *Sci. Rep.* **2025**, *15*, 27799. [CrossRef] [PubMed]
3. Alsaiari, R.A.; Kamel, M.M.; Mohamed, M.M. Corrosion inhibition of expired cefazolin drug on copper metal in dilute hydrochloric acid solution: Practical and theoretical approaches. *Molecules* **2024**, *29*, 1157. [CrossRef] [PubMed]
4. Almashhadani, H.A. Adsorption, thermodynamic and corrosion study of enalapril malate pharmaceutical drug as corrosion inhibitor for carbon steel in saline solution. *Results Mater.* **2025**, *26*, 100706. [CrossRef]
5. Bashir, S.H.; Motawea, M.M.; Younes, A.A.; Satti, A.A.; Daoub, R.M.; Atia, M.F. Utilizing expired Duloxetine as an eco-friendly corrosion inhibitor for API 5L X52 carbon steel in aqueous solutions: Experimental and computational analysis. *Results Chem.* **2025**, *16*, 102476. [CrossRef]
6. Chen, L.-M.; Li, S.-J.; Mo, J.-L.; Chen, L.-Y.; Li, H.-Z.; Guo, X.-P.; Liao, B.-K. One Stone four birds: Expired butylphthalide drugs as a high-efficient corrosion inhibitor for mild steel in acidic media. *J. Taiwan Inst. Chem. Eng.* **2026**, *180*, 106472. [CrossRef]
7. Alnahas, F.; Yeboah, P.; Fliedel, L.; Abdin, A.Y.; Alhareth, K. Expired medication: Societal, regulatory and ethical aspects of a wasted opportunity. *Int. J. Environ. Res. Public Health* **2020**, *17*, 787. [CrossRef] [PubMed]
8. Kumar, N.; Anunay, P.; Kumar, S.; Meena, L.K.; Singh, D. An overview on emerging green organic corrosion inhibitors: Sustainable solution for oil and gas industrial applications. *RSC Adv.* **2026**, *16*, 3909–3948. [CrossRef] [PubMed]
9. Zheng, Z.-J.; Trinchi, A.; Meng, X.-B.; Gao, Y. Effect of bimodal microstructure on electrochemical corrosion behavior of 304 stainless steel in 0.5 M H_2SO_4 solution. *Sci. Adv. Mater.* **2019**, *11*, 1275–1284. [CrossRef]
10. Verma, C.; Singh, A.; Singh, P.; Rhee, K.Y.; Alfantazi, A. Regioisomeric effect of heteroatoms and functional groups of organic ligands: Impacts on coordination bonding and corrosion protection performance. *Coord. Chem. Rev.* **2024**, *515*, 215966. [CrossRef]
11. Iroha, N.B.; Maduelosi, N.J.; Nnanna, L.A. The impact of tizanidine on E24 carbon steel corrosion inhibition in oilfield acidizing solution: Experimental and quantum chemical studies. *Emergent Mater.* **2023**, *6*, 137–146. [CrossRef]

12. Gunasekaran, M.; Srinivasan, P.; Mohan, K.; Sheit, H.M.K.; Rathi, V.; Vanchinathan, S. Expired pharmaceutical compounds as green corrosion inhibitors for low carbon steel in acidic conditions. *Discov. Chem.* **2025**, *2*, 338. [CrossRef]
13. Saleh, M.G.; Felaly, R.N.; Hawsawi, H.; Al-Juaid, S.S.; Elyan, S.S.; Abdallah, M.; Mustafa, S.K.; El Wanees, S.A. Inhibition efficacy of expired citalopram drug towards the damage of C-steel in hydrochloric acid solution. *Sci. Rep.* **2026**, *16*, 11619. [CrossRef] [PubMed]
14. Raghavendra, N.; Chapi, S.; Mv, M.; Pawlak, M.; Saeb, M.R. Sustainable corrosion inhibitors from pharmaceutical wastes: Advancing energy-efficient chemistry with green solutions. *Energies* **2025**, *18*, 224. [CrossRef]
15. Deiab, G.A.; Alqudah, A.; Aljaber, A.; Al-Taber, S.; Mizyed, S.; Avina, M.M.; Qanis, E.; Gammoh, O.S. Synthesis, Characterization, and In Vivo Evaluation of Escitalopram Analogues for Depression. *Russ. J. Bioorg. Chem.* **2023**, *49*, 1467–1474. [CrossRef]
16. Ikeuba, A.I.; Faithpraise, F.O.; Nwokolo, K.I.; Umo, F.E.; Echem, O.C.; Ibrahim, A.T.; Edet, H.O.; Ita, B.I.; Okafor, P.C.; Asogwa, F.C.; et al. A combined electrochemical and DFT investigation of ornidazole as a benign anti-corrosion agent for carbon steel materials in acidizing environments. *Results Mater.* **2024**, *21*, 100542. [CrossRef]
17. Hameed, R.A.; Aleid, G.M.; Khaled, A.; Mohammad, D.; Aljuhani, E.H.; Al-Mhyawi, S.R.; Alshammary, F.; Abdallah, M. Expired dulcolax drug as corrosion inhibitor for low carbon steel in acidic environment. *Int. J. Electrochem. Sci.* **2022**, *17*, 220655. [CrossRef]
18. Andrawis, M.; Ellison, L.C.; Riddle, S.; Mahan, K.; Collins, C.D.; Brummond, P.; Carmichael, J. Recommended quality measures for health-system pharmacy: 2019 update from the Pharmacy Accountability Measures Work Group. *Am. J. Health-Syst. Pharm.* **2019**, *76*, 874–887. [CrossRef] [PubMed]
19. Kotabagi, S.D.; Rajappa, S.; Minagalavar, R.L.; Rathod, M.R.; Suma, J.; Sajjan, A.M. Expired Lircetam drug as a corrosion inhibitor for low-carbon steel in 1 M HCl: Experimental, theoretical, and quantum chemical insights. *Results Surf. Interfaces* **2025**, *18*, 100459. [CrossRef]
20. Onyeachu, I.B.; Abdel-Azeim, S.; Chauhan, D.S.; Quraishi, M.A. Electrochemical and computational insights on the application of expired metformin drug as a novel inhibitor for the sweet corrosion of C1018 steel. *ACS Omega* **2020**, *6*, 65–76. [CrossRef] [PubMed]
21. Baboian, R. *Corrosion Tests and Standards: Application and Interpretation*; ASTM International: West Conshohocken, PA, USA, 2005; Volume 20.
22. Haque, J.; Srivastava, V.; Chauhan, D.S.; Quraishi, M.; Kumar, A.M.; Lgaz, H. Electrochemical and surface studies on chemically modified glucose derivatives as environmentally benign corrosion inhibitors. *Sustain. Chem. Pharm.* **2020**, *16*, 100260. [CrossRef]
23. Nasr, D.N.; El-Hossiany, A.; Khaled, M.A.; Salem, A.M.; Fouda, A. Corrosion Inhibition of expired dogmatil drug on carbon steel in HCl solution: Experimental and theoretical approaches. *Biointerface Res. Appl. Chem.* **2024**, *14*, 1–21. [CrossRef]
24. Sharma, S.; Rajpurohit, H.; Sonwal, C.; Bhandari, A.; Choudhary, V.; Jain, T. Zero order spectrophotometric method for estimation of escitalopram oxalate in tablet formulations. *J. Young Pharm.* **2010**, *2*, 420. [CrossRef] [PubMed]
25. Ishii, F.; Matsunami, S.; Shibata, M.; Kakuchi, T. UV-vis absorption study of cis-and trans poly (phenylacetylene) s based on CNDO/S calculation. *Polym. J.* **1999**, *31*, 84–88. [CrossRef]
26. Sheladia, S.; Patel, B. Determination of escitalopram oxalate and L-methylfolate in tablet by spectrophotometric and reverse phase high-performance liquid chromatographic methods. *J. Chromatogr. Sci.* **2017**, *55*, 550–555. [CrossRef] [PubMed]
27. Singh, R.; Mendhulkar, V.D. FTIR studies and spectrophotometric analysis of natural antioxidants, polyphenols and flavonoids in Abutilon indicum (Linn) sweet leaf extract. *J. Chem. Pharm. Res.* **2015**, *7*, 205–211.
28. Alkahtani, M.E.; Aodah, A.H.; Abu Asab, O.A.; Basit, A.W.; Orlu, M.; Tawfik, E.A. Fabrication and characterization of fast-dissolving films containing escitalopram/quetiapine for the treatment of major depressive disorder. *Pharmaceutics* **2021**, *13*, 891. [CrossRef] [PubMed]
29. Kanagathara, N.; Shenbagarajan, P.; Jeyanthi, C.E.; Thirunavukkarasu, M. Fourier transform infrared spectroscopic investigation on Nifidipine. *Int. J. Pharm. Biol. Sci.* **2011**, *1*, 52–56.
30. Zghari, B.; Doumenq, P.; Romane, A.; Boukir, A. GC-MS, FTIR and 1H, 13C NMR structural analysis and identification of phenolic compounds in olive mill wastewater extracted from oued Oussefrou effluent (Beni Mellal-Morocco). *J. Mater. Environ. Sci.* **2017**, *8*, 4496–4509. [CrossRef]
31. El-Haddad, M.N.; Fouda, A.; Hassan, A. Data from chemical, electrochemical and quantum chemical studies for interaction between Cephapirin drug as an eco-friendly corrosion inhibitor and carbon steel surface in acidic medium. *Chem. Data Collect.* **2019**, *22*, 100251. [CrossRef]
32. Toghan, A.; Alduaij, O.K.; Attia, A.; Al Bahir, A.; Masoud, E.M.; Alhussain, H.; Eldesoky, A.M.; Farag, A.; Fawzy, A. Engineering, Exploring the inhibitory performance of expired moxifloxacin and norfloxacin on copper corrosion in saline environment. *J. Electrochem. Sci. Eng.* **2025**, *15*, 2464. [CrossRef]
33. Annon, I.A.; Abbas, A.S.; Al-Azzawi, W.K.; Hanoon, M.M.; Alamiery, A.; Isahak, W.N.R.; Kadhum, A.A.H. Corrosion inhibition of mild steel in hydrochloric acid environment using thiadiazole derivative: Weight loss, thermodynamics, adsorption and computational investigations. *S. Afr. J. Chem. Eng.* **2022**, *41*, 244–252. [CrossRef]

34. Geethamani, P.; Kasthuri, P. The inhibitory action of expired asthalin drug on the corrosion of mild steel in acidic media: A comparative study. *J. Taiwan Inst. Chem. Eng.* **2016**, *63*, 490–499. [CrossRef]
35. Saxena, A.; Kaur, J.; Mutreja, V.; Yadav, K.K.; Obaidullah, A.J.; Katin, K.P.; Berdimurodov, E.; Verma, D.K. Gravimetric, electrochemical, surface morphological, and simulation studies of the use of expired Meftal-P drug as a novel anti-corrosive coating material for steel in 0.5 M HCl. *Eur. Phys. J. Plus* **2025**, *140*, 471. [CrossRef]
36. Pang, X.; Ran, X.; Kuang, F.; Xie, J.; Hou, B. Inhibiting effect of ciprofloxacin, norfloxacin and ofloxacin on corrosion of mild steel in hydrochloric acid. *Chin. J. Chem. Eng.* **2010**, *18*, 337–345. [CrossRef]
37. Shoair, A.G.F.; Motawea, M.M.; Almalki, A.S.; Shanab, M.M.; El-Basiony, A.; Nasef, H.A. Expired terazosin as environmentally safe corrosion inhibitor for 1018 carbon steel in 1 M HCl solution: Experimental and computational studies. *Int. J. Electrochem.* **2024**, *19*, 100397. [CrossRef]
38. Subri, N.W.B.; Sarraf, M.; Nasiri-Tabrizi, B.; Ali, B.; Sabri, M.F.M.; Basirun, W.J.; Sukiman, N.L. Corrosion Insight of Iron and Bismuth Added Sn–1Ag–0.5Cu Lead-Free Solder Alloy. *Corros. Eng. Sci. Technol.* **2020**, *55*, 35–47. [CrossRef]
39. Rotaru, I.; Varvara, S.; Gaina, L.; Muresan, L.M. Antibacterial drugs as corrosion inhibitors for bronze surfaces in acidic solutions. *Appl. Surf. Sci.* **2014**, *321*, 188–196. [CrossRef]
40. Tan, B.; Ren, H.; Yin, C.; Li, X.; Li, X.; Wang, R.; Guo, L.; Zhang, Y.; Al-Sadoon, M.K. *Nepeta cataria* L. leaf extracts as eco-conscious corrosion inhibitor for copper in H_2SO_4 medium. *Colloids Surf. A Physicochem. Eng. Asp.* **2025**, *711*, 136399. [CrossRef]
41. Zhao, H.; Deng, S.; Qiang, Y.; Xu, J.; Xu, D.; Li, X. Synergistic mixture of Camellia Oleifera shell extract and KI as an eco-friendly and highly efficient composite inhibitor for steel corrosion in H_2SO_4 media. *J. Mol. Liq.* **2024**, *407*, 125164. [CrossRef]
42. Sheit, H.M.K.; Kani, S.M.; Sathiq, M.A.; Abuthahir, S.S.; Subhapriya, P.; Nivedhitha, K.; Umarfarooq, M.; Badruddin, I.A.; Kamangar, S.; Shaik, A.S. Experimental studies on the effect of expired Amiodarone drug (EAD) as a corrosion inhibitor on mild steel in 1 M HCl. *Materials* **2024**, *17*, 751. [CrossRef] [PubMed]
43. Ali, B.; Mohd Sabri, M.F.; Mohd Said, S.; Sukiman, N.L.; Jauhari, I.; Soin, N. High impact reliability and high temperature performance of Fe and Bi added Sn-1Ag-0.5 Cu solder alloys. *J. Mater. Sci. Mater. Electron.* **2017**, *28*, 7277–7285. [CrossRef]
44. Ali, B.; Mohd Sabri, M.F.; Sukiman, N.L.; Jauhari, I. Microhardness and shear performance of Fe/Bi-bearing SAC105 solder alloys under high temperature aging. *J. Mater. Sci. Mater. Electron.* **2017**, *28*, 197–206. [CrossRef]
45. Obot, I.; Macdonald, D.; Gasem, Z. Density functional theory (DFT) as a powerful tool for designing new organic corrosion inhibitors. Part 1: An overview. *Corros. Rev.* **2015**, *99*, 1–30. [CrossRef]
46. Geerlings, P.; De Proft, F.; Langenaeker, W. Conceptual density functional theory. *Chem. Rev.* **2003**, *103*, 1793–1874. [CrossRef] [PubMed]
47. Fouda, A.; Abdel-Wahed, H.; Atia, M.; El-Hossiany, A. Novel porphyrin derivatives as corrosion inhibitors for stainless steel 304 in acidic environment: Synthesis, electrochemical and quantum calculation studies. *Sci. Rep.* **2023**, *13*, 17593. [CrossRef] [PubMed]
48. Farhadian, A.; Zhao, Y.; Naeiji, P.; Rahimi, A.; Berisha, A.; Zhang, L.; Rizi, Z.T.; Iravani, D.; Zhao, J. Simultaneous inhibition of natural gas hydrate formation and CO_2/H_2S corrosion for flow assurance inside the oil and gas pipelines. *Energy* **2023**, *269*, 126797. [CrossRef]
49. Fu, Y.; Huang, C.; Du, C.; Li, J.; Dai, C.; Luo, H.; Liu, Z.; Li, X. Evolution in microstructure, wear, corrosion, and tribo corrosion behavior of Mo-containing high-entropy alloy coatings fabricated by laser cladding. *Corros. Sci.* **2021**, *191*, 109727. [CrossRef]
50. Lebrini, M.; Lagrenée, M.; Vezin, H.; Traisnel, M.; Bentiss, F. Experimental and theoretical study for corrosion inhibition of mild steel in normal hydrochloric acid solution by some new macrocyclic polyether compounds. *Corros. Sci.* **2007**, *49*, 2254–2269. [CrossRef]
51. Emrayed, H.F.; Mohammed, N.A.; Khatab, H.A.; Ali, A.M.; Kirallah, N.F.; Adress, H.M.; Fouda, A.E.-A.S. Recycling of expired Ceporex drug (CPX) as a corrosion inhibitor for carbon steel in a hydrochloric acid medium. *RSC Adv.* **2026**, *16*, 35090. [CrossRef] [PubMed]
52. Tsygankova, L.; Bryaksina, V.; Uryadnikov, A.; Kanaeva, L. Using expired drotaverine for corrosion protection of steel in HCl solution. *Chem. Bull. Kazakh Natl. Univ.* **2025**, *115*, 24–30.
53. Popović, A.S.; Aligayev, A.; Trajković, D.V.; Jovanović, G.; Rakočević, L.; Grgur, B.N. Coupled experimental and theoretical investigation of an antidiabetic drug as a green corrosion inhibitor for low-carbon steel in acidic media. *J. Electroanal. Chem.* **2026**, *1011*, 120076. [CrossRef]
54. Fouda, A.; El-Ewady, G.; Ali, A. Modazar as promising corrosion inhibitor of carbon steel in hydrochloric acid solution. *Green Chem. Lett. Rev.* **2017**, *10*, 88–100. [CrossRef]
55. Omar, H.M.; Ankah, N.; Gomaa, M.S.; Alkhaldi, M.Y.; Osman, N.M.; Al-Subaie, A.R.; Aldossary, I.; Baig, I.; Bahraq, A.A.; Aljohani, M.; et al. Towards a Sustainable Material Protection: Olanzapine Drugs and Their Derivatives as Corrosion Inhibitors for C1018 Steel in 1 M Hydrochloric Acid. *Materials* **2025**, *18*, 2902. [CrossRef] [PubMed]
56. Dohare, P.; Chauhan, D.; Quraishi, M. Expired Podocip drug as potential corrosion inhibitor for carbon steel in acid chloride solution. *Int. J. Corros. Scale Inhib.* **2018**, *7*, 25–37. [CrossRef]

57. Al-Nami, S.Y. Corrosion inhibition of low carbon steel in 1 M HCl solution by cephalexin monohydrate drug and synergistic iodide additives. *Biointerface Res. Appl. Chem.* **2021**, *11*, 8550–8563. [CrossRef]
58. Kalkhambkar, A.G.; Rajappa, S.; Manjanna, J. Evaluation of corrosion inhibition efficiency of cefpodoxime proxetil expired drug for low carbon steel in 1 M HCl solution. *Next Res.* **2025**, *2*, 100194. [CrossRef]
59. Satti, A.A.; Younes, A.A.; Shanab, M.M.; Bashir, S.H.; Daoub, R.M.A.; Motawea, M.M.; Eissa, M.E. Recycling pharmaceutical waste (vancomycin) as sustainable corrosion inhibition for API 5 L X60 carbon steel in 1 M hydrochloric acid: A combined electrochemistry and theoretical study. *Sci. Rep.* **2026**, *16*, 23459. [CrossRef] [PubMed]
60. Abd El Maksoud, S.; Fouda, A.E.A.; Badawy, H. Furosemide drug as a corrosion inhibitor for carbon steel in 1.0 M hydrochloric acid. *Sci. Rep.* **2024**, *14*, 9052. [CrossRef] [PubMed]

Disclaimer/Publisher's Note: The statements, opinions and data contained in all publications are solely those of the individual author(s) and contributor(s) and not of MDPI and/or the editor(s). MDPI and/or the editor(s) disclaim responsibility for any injury to people or property resulting from any ideas, methods, instructions or products referred to in the content.